Renewable Energy 58 (2013) 50–59

Contents lists available at SciVerse ScienceDirect

Renewable Energy

journal homepage: www.elsevier.com/locate/renene

A study on the effect of different modeling parameters on the dynamic response of a jacket-type offshore wind turbine in the Korean Southwest Sea

Wei Shi [a], Hyunchul Park [b], Jonghoon Han [c], Sangkwon Na [d], Changwan Kim [a,*]

[a] School of Mechanical Engineering, Konkuk University, Seoul 143-701, Republic of Korea
[b] Graduate School of Wind Energy, POSTECH, Pohang, Kyungbuk 790-784, Republic of Korea
[c] Central R&D Institute, Daewoo Shipbuilding & Marine Engineering Co., Ltd, Seoul 135-010, Republic of Korea
[d] Research Institute of Industry Science and Technology, Incheon 406-840, Republic of Korea

ARTICLE INFO

Article history:
Received 5 September 2012
Accepted 9 March 2013
Available online 1 April 2013

Keywords:
Offshore wind turbine
Jacket foundation
Dynamic response
Modeling parameters

ABSTRACT

As a country mostly surrounded by water, Korea has good potential for offshore wind energy utilization. With offshore wind turbines growing larger and with increasing water depth, jacket structures are attracting increased attention because they appear to be cost-effective, but they are still at an early stage of development for use in the offshore wind industry. This paper aims to design a jacket structure to support a 5 MW wind turbine in 33 m deep water for a Korean offshore demonstration project and to investigate the effects of different modeling parameters (including joint can, overlap, flooding of the member, marine growth and mass of the transition piece) on the dynamic response of an offshore wind turbine with a jacket substructure. For this purpose, modal analysis and aero-servo-hydro-elastic simulation with varying modeling parameters are performed under Korean environmental conditions. The results show that joint can, overlap and marine growth strongly affect the dynamic response and there is a small effect on the natural frequencies of the designed structure. Choosing the appropriate transition piece mass may reduce the extreme loads in the members. This study provides applicable knowledge of the utilization of large-scale offshore wind turbines for intermediate water depths in Korea.

1. Introduction

In response to the energy crisis and the greenhouse effect, wind energy has become the most cost-effective of all currently exploited renewable energy sources [1]. Various studies have been conducted on wind energy [2–4]. In recent years, offshore wind energy has attracted more attention due to better wind conditions and negligible visual impact compared with onshore wind energy. Although offshore wind energy has experienced rapid development, there is still a growing global demand for wind energy production [5,6]. As the 13th largest economy relying on imported sources for 97% of its energy needs, South Korea will invest 10.2 trillion won (US$9 billion) in building a 2.5 GW offshore wind farm in the Korean Southwest Sea by 2019 [7].

The type of support structure for an offshore wind turbine (OWT) depends mainly on water depth, turbine size, and met ocean and soil conditions. To date, most wind turbines have been installed with monopile or gravity foundations in shallow water, and these solutions may be stretched to deeper water and larger wind turbines. Gravity-based substructures are used for 5 MW turbines in water depths of up to 27 m for the Thornton Bank wind farm in Belgium [8], and the feasibility of monopile foundation for 5 MW turbines in water depths up to 30 m was discussed by Seidel [9]. As OWTs grow larger and the water depth increases at the installation locations, monopile or gravity foundations may not be economically viable or technically feasible. Therefore, with the aid of technologies from the oil and gas industries, hydrodynamic transparent space-frame support structures such as tripods, jackets or tripiles are currently used in several EU projects. Two types of 5 MW turbines were used in the German Alpha Ventus wind farm atop tripods and jackets in 30 m deep water[10]. Jackets were used in the Beatrice Demonstrator Project [11]at a water depth of 45 m, while tripiles are currently installed in 40 m deep water in the BARD offshore 1 project in Germany [12], but jacket structures are still at an early stage of development for application in the offshore wind industry.

Reliable and cost-effective OWTs with jacket structures are designed and certified based on accurate and detailed predictions of loads and dynamic responses calculated in aero-servo-hydro-elastic (or fully coupled) simulations. Decoupled or integrated analysis was

* Corresponding author. Tel.: +82 2 450 3543; fax: +82 2 447 5886.
E-mail address: goodant@konkuk.ac.kr (C. Kim).

0960-1481/$ – see front matter © 2013 Elsevier Ltd. All rights reserved.
http://dx.doi.org/10.1016/j.renene.2013.03.010

conducted to study the wind turbine behavior and structural dynamics of the jacket support structures in the earlier studies[13–16]. However, few studies have focused on the effect of modeling parameters such as joint can, overlap and marine growth on the dynamic response of jacket substructures. Fischer et al. [17] evaluated the effect of availability, corrosion and marine growth on the fatigue loading of the jacket support structure. Moll et al. [18] proved that adding hydrodynamic masses has a significant effect on frequencies, and to get the most precise results, added masses need to be considered when performing a dynamic analysis of an OWT. The joint can and overlap effects were studied in [19,20], respectively. The marine growth effect was studied a little in previous work [21].

In spite of the OWT with jacket foundation, no systematic study on the modeling parameters has been found in the literatures. Moreover, OWT is a site-specific design. Designing the support structures based on the local conditions is essential for Korean offshore demonstration project.

In this work, a jacket substructure for a 5 MW OWT is designed for the Korean Southwest Sea demonstration project based on local environmental conditions. In addition, the effects of different modeling parameters (including joint can, overlap, flooding of the member, marine growth and mass of the transition piece (TP)) on the dynamic response of an OWT with a jacket substructure are investigated. The results are presented in terms of mass comparison, modal analysis and fully coupled dynamic analysis. Dynamic responses are presented and compared for the selected sensors in terms of the extremes in the local coordinate system.

2. Hydrodynamic loads

OWTs are subjected to various loads, including aerodynamic loads because of wind, hydrodynamic loads because of waves and currents, and gravity and operational loads. The aerodynamic loads calculation can be found easily from other literature [22]. This section describes the theories related to hydrodynamic loads, which are the important load source for OWT.

The typical wave spectrum is represented with a height–period bin (H, T). If the entire spectrum is divided into N frequency bands with width Δf, then the water particle displacement, velocity and acceleration are obtained from:

$$\eta(t,x) = \sum_{i=1}^{N} \eta_i(t,x) = \sum_{i=1}^{N} \frac{H_i}{2} \sin(k_i x - 2\pi f_i t + \varepsilon_i) \tag{1}$$

$$u_w(t,x) = \sum_{i=1}^{N} -2\pi f_i \frac{H_i}{2} \cos(k_i x - 2\pi f_i t + \varepsilon_i) \tag{2}$$

$$\dot{u}_w(t,x) = \sum_{i=1}^{N} (2\pi f_i)^2 \frac{H_i}{2} \sin(k_i x - 2\pi f_i t + \varepsilon_i) \tag{3}$$

For a slender structure immersed in waves, if the diffraction parameter D/λ is less than 0.2, the dynamic forces on the structure can be calculated using the relative-motion Morison's equation (Eq. (4)) [23,24]. The drag and inertia components are calculated from the aforementioned water particle kinematics. The force per unit length of the member is:

$$F_{\text{Morision}} = C_m \cdot \frac{1}{4}\pi\rho D^2 \dot{u}_w - (C_m - 1)\frac{1}{4}\pi\rho D^2 \dot{u}_s + C_d \cdot \frac{1}{2}\rho D(u_w - u_s)|u_w - u_s| \tag{4}$$

where u_w is the water particle velocity and $\dot{u}_w$ is the water particle acceleration, u_s is the structure velocity, C_d is the drag coefficient, C_m is the inertia coefficient, D is the member diameter, and ρ is the density of the water.

Joint cans could increase the member diameter so that the hydrodynamic loads will increase due to the joint cans. Considering overlapping will reduce the buoyancy force and hydrodynamic force because of reduced volume of the members at the overlap part. Marine growth not only increases the diameter of the structure, but also modifies the structure surface roughness so that the hydrodynamic coefficients are also modified.

Hydrodynamic mass (or water added mass) is defined as the mass of fluid around an object which is accelerated with the acceleration of the object. It is caused due to relative acceleration between the object and the fluid. It can be determined by the integration of pressure around the object and is often expressed by:

$$m_{\text{add}} = \rho C_a V \tag{5}$$

where C_a is the added mass coefficient and V is the volume of the object. It can be proved that for a circular cylinder, $C_a = 1$. The hydrodynamic mass has been assumed to equal the mass of the displaced water volume, which is used for wave load determination on offshore structures.

3. Offshore wind turbine model and environmental conditions

3.1. Wind turbine model

The National Renewable Energy Laboratory (NREL) 5 MW offshore baseline model [25] is used for modeling the wind turbine in our study because it is a good representation of the characteristics of a typical 5 MW OWT being manufactured today. Furthermore, other research teams and international projects (UpWind project, IEA Wind Annex 23 OC3 and IEA Wind Annex 30 OC4) throughout the world have adopted it as a reference model to standardize baseline OWT specifications. The NREL 5 MW model is a conventional upwind, variable speed, collective pitch, horizontal axis wind turbine and its main dimensions and characteristics are shown in Table 3. More detailed information can be found in Jonkman's definition [25]. During the jacket design process, the hub height of the turbine is changed from 90 m to 96.6 m because of changes in the elevation of TP. The TP of the jacket is 16.6 m above the mean sea level (MSL), which is different from the NREL monopile reference (10 m above MSL). NREL DLL external controller is used in our work.

3.2. Jacket support structure

The jacket support structure is designed according to the environmental conditions described in Section 3.1 at a water depth of 33 m. The designed jacket consists of four battered legs, four central piles, four levels of X-braces, mud braces and a TP. The inclination of the battered leg is 9.9°. The height of this jacket substructure ranges from −33 m to 16.6 m above MSL. The jacket is connected by a TP to the tower bottom 16.6 m above the MSL. The upper conical tower is 77.6 m high, resulting in a hub height of 96.6 m above MSL. The base area of the jacket is 21.536 m × 21.536 m and the top area is12.323 m × 12.323 m. The piles below the mudline are rigidly cantilevered. To account for paint, bolts, welds and flanges, which are not accounted for in the thickness data, the density of the steel used in the construction of both the tower and jacket is taken to be 8500 kg/m^3; the Young's modulus and shear modulus are taken to be 2.1×10^{11} N/m^2 and

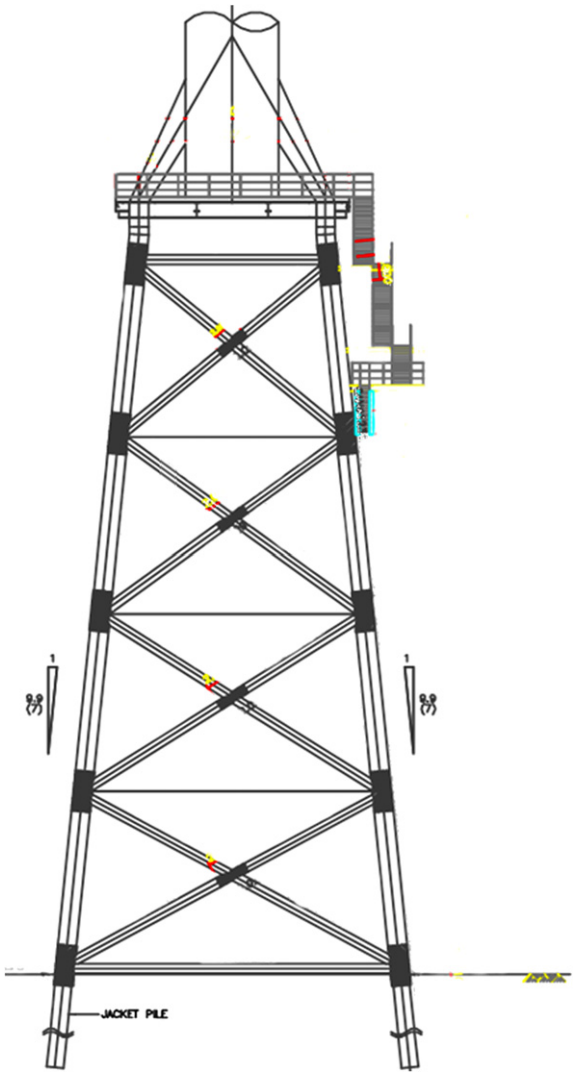

Fig. 1. Designed jacket structure in this study.

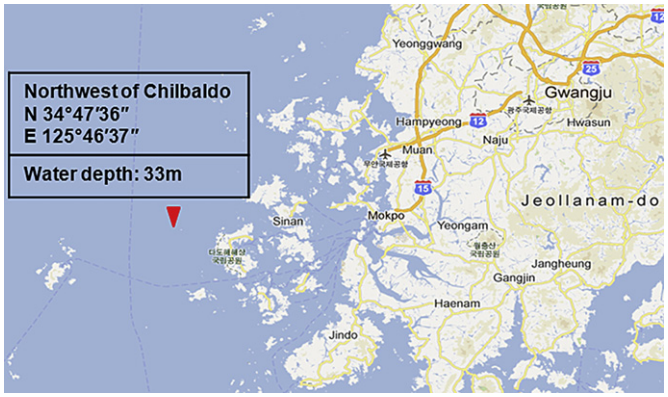

Fig. 3. Reference site in the Korean Southwest Sea.

8.077×10^{10} N/m^2, respectively. The design parameters of this jacket substructure concept are shown in Table 2.The designed jacket structure is shown in Fig. 1.

3.3. Reference site

Korea has an ambitious plan to build an offshore demonstration wind farm at a cost of US$9 billion, to be built off the southwest coast of the Korean peninsula over a period of 10 years. According to the Korean Ministry of Knowledge Economy (MKE), the project commenced in 2009 is basically composed of three phases. By 2013, 20 wind turbines rated at 5 MW will be raised; 180 more will be added by 2016; and a further 300 by 2019. The location of this demonstration project is shown in Fig. 2.

In this study, the OWT is analyzed for a site with a water depth of 33 m. The site coordinates are N34°47′36″, E125°46′37″, which is near Chilbal Island, Shinan County off the South Jeolla province. This site is located in the area of the Korean offshore demonstration wind farm, approximately 10 km from the coast (Fig. 3). Meteorological data at the selected site are measured from July 1st 1996 to December 31st 2010. Wind and wave conditions are given in Tables 1 and 2 in detail.

4. Modeling parameters

More optimized structures and cost-effective jacket structures are based on accurate and detailed predictions of loads and

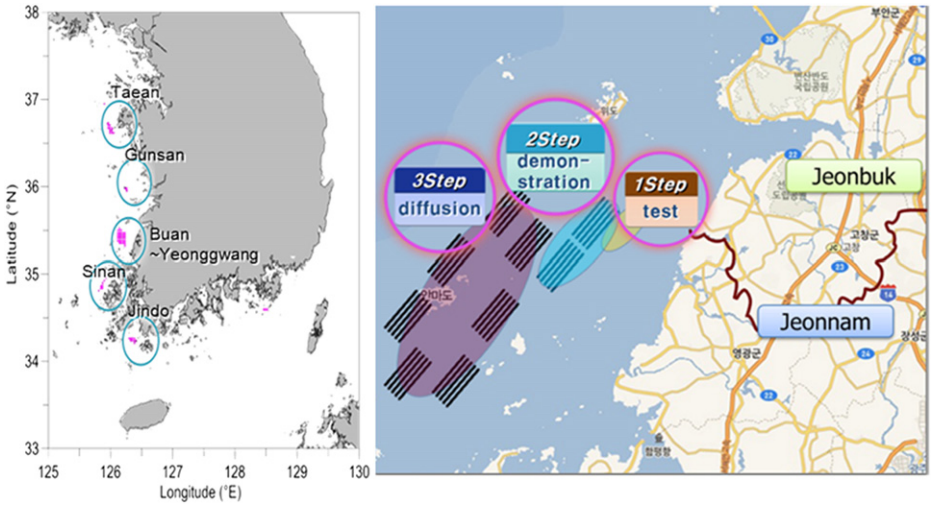

Fig. 2. Korean offshore wind demonstration project.

Table 1
Wind condition at the reference site.

Return period (year)	Wind speed (m/s)	Gust (m/s)
100	31.05	40.75
50	30.24	39.69
20	29.14	38.24
10	28.28	37.11
1	25.22	33.06
Measured average	6.87	9.24

Table 2
Wave condition at the reference site.

Return period	Maximum wave		Significant wave		Average wave	
	Height (m)	Period (s)	Height (m)	Period (s)	Height (s)	Period (s)
100	6.76	12.79	4.06	10.00	1.96	6.79
50	6.58	12.62	3.95	9.74	1.91	6.79
10	6.16	12.36	3.70	9.54	1.79	6.62
1	5.49	11.57	3.30	8.95	1.60	6.03
Measured average	1.40		0.83		0.39	5.14

Table 3
Properties of jacket members.

Component	Diameter (m)	Thickness (mm)
Leg	1.2192	25.4
Joint can	1.2319	38.1
X-braces	0.609	12.7
Brace can	0.609	25.4

dynamic responses calculated in aero-servo-hydro-elastic simulations. Different modeling techniques play important roles in the accuracy of simulations. In this study, the effect of modeling parameters, including joint can, overlap, flooding of the member, marine growth and TP mass, are investigated by modal analysis and time domain fully coupled dynamic analysis.

4.1. Joint can

Compared with their monopile and gravity-based counterparts, a number of features are unique to jacket structures. In particular, there are joint cans, especially around the X-joints, to match the code check requirements (Fig. 4(a)). Joint can properties differ from basic tube properties in terms of increased diameters and wall thicknesses (Fig. 4(b) and (c)). A comparison study is performed using the jacket support structure designed in Section 3.3 with and without joint cans.

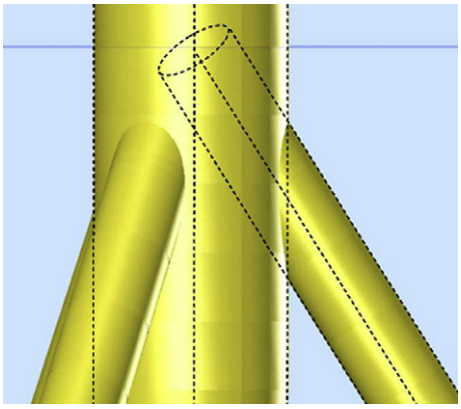

Fig. 5. Schematic diagram of overlap in jacket structure.

4.2. Overlap

For the jacket structure, the connecting nodes of elements at joints are defined at the intersection points of the members' centerlines and this leads to overlap of elements in the analyzed jacket (Fig. 5). If they are not properly modeled, the significant surface areas and volumes are duplicated, distorting the overall level of wave and buoyancy loading. The intersecting members will also have an effect on the mass of the jacket.

4.3. Flooding of the member

When the jacket structure is erected offshore, the legs of the jacket below the sea surface are immersed in the sea and flooded with seawater (Fig. 6). The member is considered to be sealed in this study. For the sealed member with flooded, the buoyancy is the

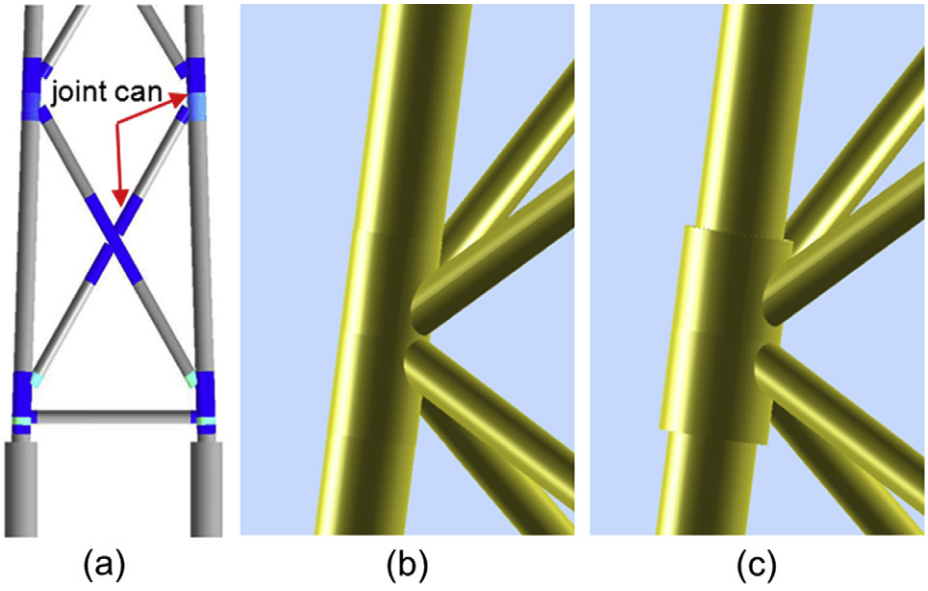

Fig. 4. Schematic diagram of joint can in jacket structure.

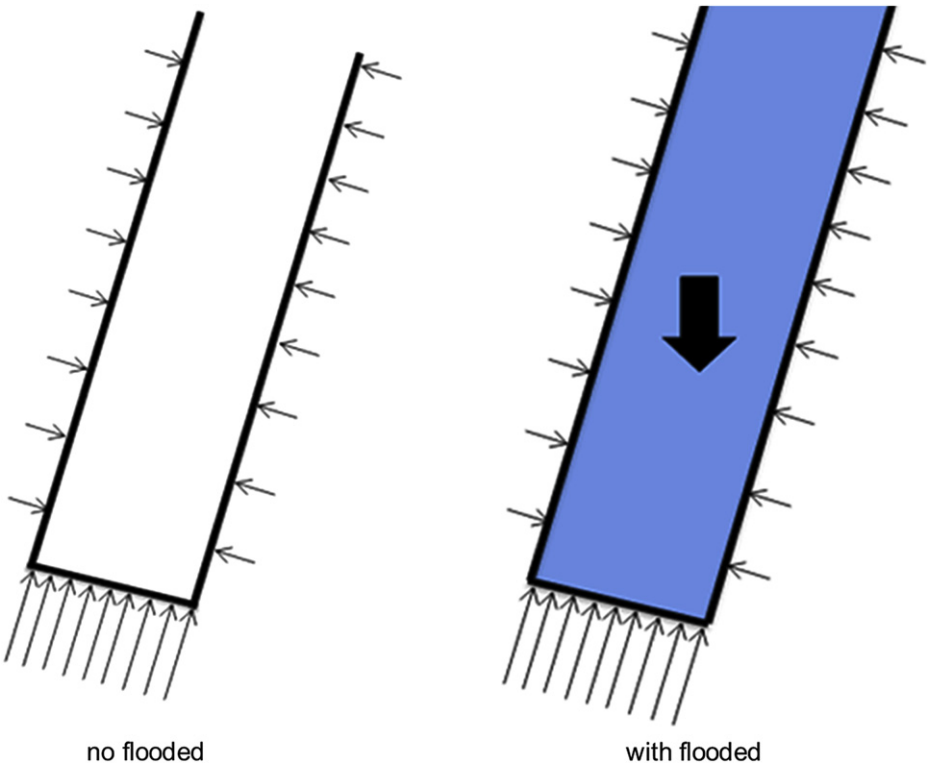

Fig. 6. Schematic diagram of flooded member in jacket structure.

water displaced by the submerged member based on its outer diameter. For the unsealed member, if it is flooded, the buoyancy is only the water displaced by the volume of the member self. The results are presented with and without flooded members.

4.4. Marine growth

Numerous types of marine fouling organisms may be found on the submerged members of the jacket (Fig. 7). For offshore structures such as jackets or jack-up platforms, the hydrodynamic overloading caused by marine growth is a major concern in terms of the percentage on each component, and consequently on their summation for the external global loading assessment. Marine growth has caused an increase in the cross-sectional area for all underwater members of offshore structures, and changes in surface roughness. The increase of surface roughness leads to the increase of the drag coefficient, C_d, and the decrease of the inertia coefficient, C_m. As recommended by Det Norske Veritas (DNV) guidelines

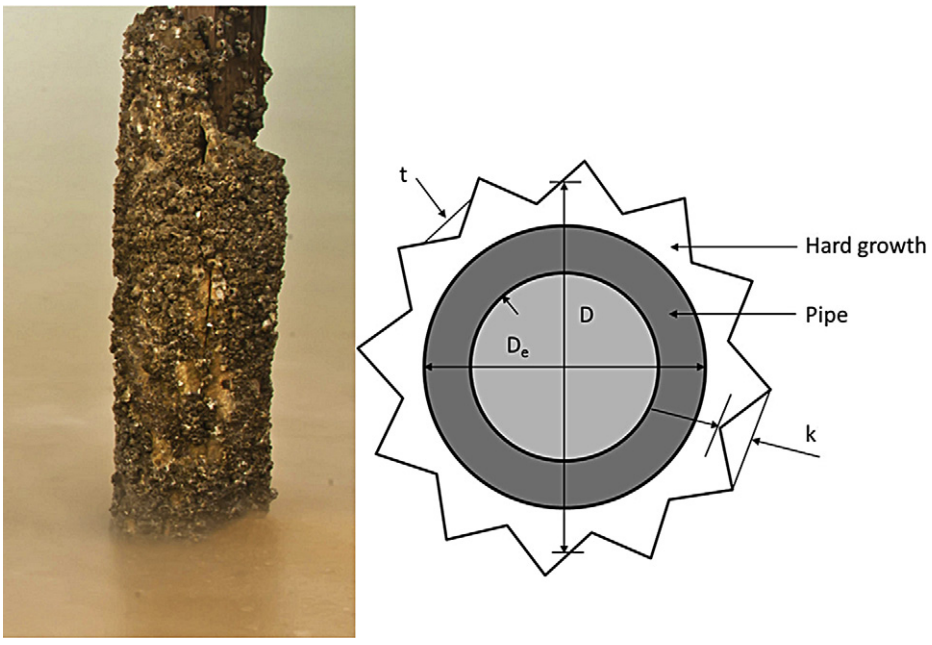

Fig. 7. Schematic diagram of marine growth in jacket structure.

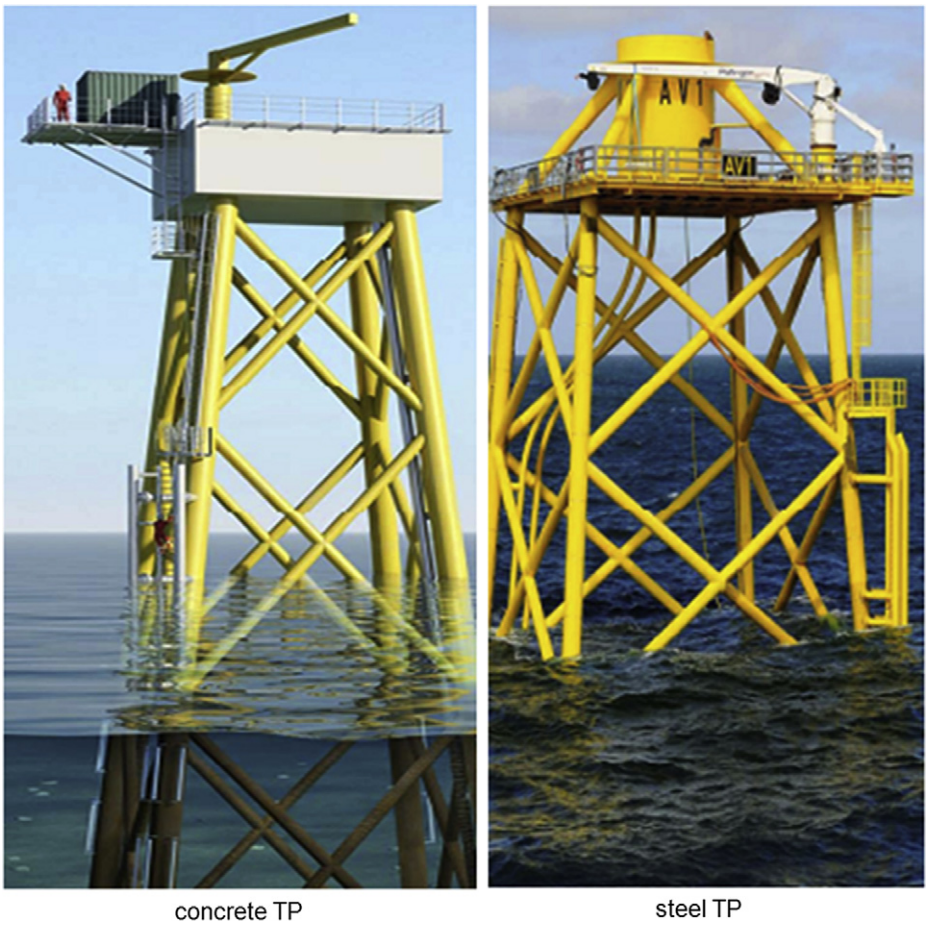

Fig. 8. Different TP models.

[26], the marine growth is present from the seabed to a water depth of 2 m at a density of 1100 kg/m^3 and a thickness of 100 mm. Hydrodynamic coefficients, $C_d = 1.0$, $C_m = 2.0$ are used for the case without marine growth. And $C_d = 1.2$, $C_m = 1.8$ are used for the case with marine growth. So the hydrodynamics and mass of the tower member are affected by the marine growth. But it doesn't affect the stiffness of the structure.

4.5. Mass of TP

For OWTs, jacket structures are used as substructures supporting the monotower and are designed for 5 MW turbines with a rotor nacelle assembly (RNA) mass of around 350–410 tons. During the design process, there is a critical connection between the jacket structure and the tower – the transition piece. Although the design of the TP varies according to specific and individual project requirements including the loading conditions, connecting structure dimensions, RNA weight, etc., the general types of TPs include a heavy concrete block (UpWind project) and lightweight frame-cylinder design (Beatrice and Alpha Ventus projects) (Fig. 8). Three different masses are used in this work to study the effect of TP mass. The TP mass is similar to the REpower model (22% of the support structure) in model 1, to the UpWind design (43% of the support structure) in model 3, and mass of TP is between models 1 and 3 in model 2.

Table 4
Design load case.

Degree of freedom	All-platform, tower, drive train, blades
Wind condition	Turbulent wind (Mann model), $V_{hub} = 11.4$ m/s, $\sigma_1 = 1.68$ m/s
Wave condition	NSS: irregular wave (JONSWAP), $H_s = 8$ m, $T_p = 10$ s
Current speed	1.6 m/s
Inertial conditions	Rot speed = 12.1 rpm, azimuth = 0 deg (blade 1 up), pitch = 0°
Other conditions	Wind, wave and current directions are assumed fully aligned and are applied along the jacket foundation

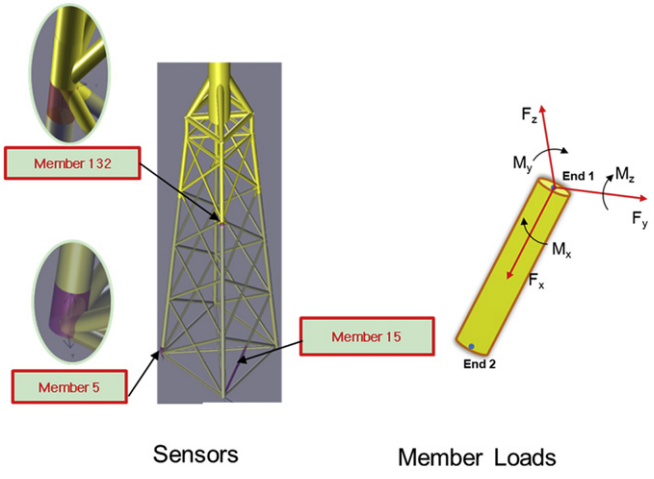

Fig. 9. Location of output sensors.

Table 5
Mass comparison due to joint can effect (unit: ton).

	No joint can	With joint can	Difference
Mass of support structure	1006.5	1039.5	3.28%

Table 6
Tower natural frequencies due to joint can effect (unit Hz).

Mode	No joint can	With joint can	Difference (%)
1	0.2407	0.2417	0.42
2	0.2416	0.2426	0.41
3	1.8900	1.7720	−6.24
4	2.0663	3.1198	50.9
5	3.4045	3.4155	0.32

5. Design load case

To investigate the effect of modeling parameters described in Section 4, an exemplary time domain load case is defined according to the environmental conditions outlined in Section 3.3 as follows (a 50-year return period was chosen). The design load case is defined in Table 4 in detail.

In this work, the structural damping, hydrodynamic damping and aerodynamic damping (the controller can also add damping) are included. The structural damping is applied to each mode of the flexible component. Hydrodynamic damping from viscous forces is applied as external loads.

A large number of output parameters relate to the loads and deflection of the blade, drivetrain, generator, tower and support structure. Therefore, only the loads related to jacket foundation are presented. The typical positions for the output sensors that are analyzed are shown in Fig. 9. The loads at these positions includes the axial force and bending moments of pile 1 at the mudline (member 5), the axial force and bending moment of the upwind brace at the very bottom X-joint (member 15) and the axial force and bending moment in leg 2 at the first K-joint (member 132). The forces at the members are the dynamic response, including the inertia forces and damping forces. Each member is defined with its own local coordinate system (Fig. 9). The local x-axis is defined along the member axis, in the direction from End 1 to End 2. The z-axis is defined according to the member direction cosine. The local member y-axis is in the horizontal plane, with the z-axis forming a right-hand coordinate system. Thus, F_x is the member's axial force, F_y and F_z are the shear forces and M_x is the torsional bending moment, whereas M_y and M_z are the bending moments.

6. Numerical results and discussion

In this section, the effects of different modeling parameters on the dynamic response of the designed jacket structure are investigated. The results are presented in terms of mass comparison, the tower's natural frequency and extremes for each of the modeling parameters discussed in Section 4. Here, the tower's natural frequency refers to the coupled natural frequencies related to the support structure, which includes the tower, TP and jacket structure.

6.1. Effect of joint can

The joint cans are modeled by increasing the diameter and thickness of the member. Table 5 shows that because of the joint can, the jacket mass increased by around 33.0 tons, accounting for 3.28% of the support structure.

The first five coupled natural frequencies related to support structures are compared in Table 6 for the model with and without the joint can. The largest difference occurs for the fourth tower mode (51.64%). The mode shapes are not the same with joint can and without joint can. For the model without joint can, the mode is second tower fore-aft mode. For the model with joint can, the mode is second tower side-to-side mode (Fig. 10). There is little effect on the other frequencies.

Table 7 presents the extreme values for the selected member loads. The shear forces, F_y and F_z, and the torsional moment, M_x, have relatively small absolute values compared with other loads, and therefore are not presented. The differences between results with and without the joint can are obviously significant for some of the values, such as the axial force F_x and the bending moments M_y and M_z. Modeling with the joint can led to increased extremes lying between 2.07% and 56.72% comparing with can model. A larger difference is shown for bending moment M_y.

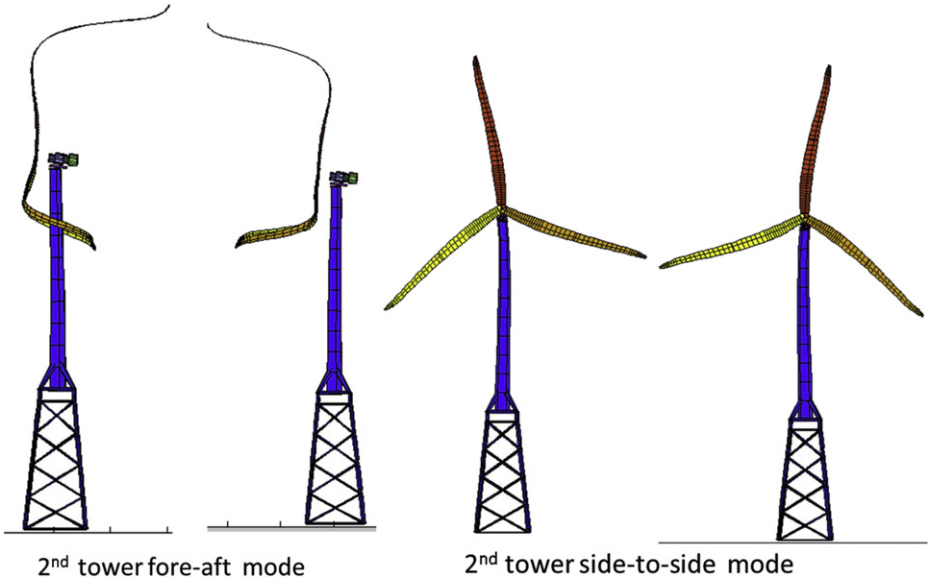

Fig. 10. Second fore-aft and side-to-side mode shapes of support structures.

Table 7
Extreme values due to joint can effect (kN or kNm).

Location	Load	No joint can	With joint can	Difference (%)
M5E1	F_x	−5797.9	−6045.7	4.27
	M_y	91.5	143.4	56.72
	M_z	135.8	152.0	11.93
M15E2	F_x	−198.0	−193.9	−2.07
	M_y	8.8	10.8	22.73
	M_z	−5	−4.7	−6.00
M132E1	F_x	−1545.6	−1668.9	7.98
	M_y	−143.4	−162.4	13.25
	M_z	110.1	116.4	5.72

Table 8
Mass comparison due to overlap effect (unit: ton).

	No overlap	With overlap	Difference (%)
Mass of support structure	938.8	1039.5	10.73

Table 9
Tower natural frequencies due to overlap effect (unit Hz).

Mode	No overlap	With overlap	Difference (%)
1	0.2356	0.2417	2.59
2	0.2365	0.2426	2.58
3	1.9511	1.7720	−9.18
4	3.0310	3.1198	2.93
5	3.3895	3.4155	0.77

6.2. Effect of overlap

Because of overlap, the volume and outer areas of the jacket structures are doubled at the joint. Therefore, the buoyancy force and wave load for overlapped members are overestimated. In this work, the massless beam with very small diameter is used to consider overlap. Similar and fictitious bending and shearing stiffness are assumed for overlapping compared with normal parts. The wave forces at the joints for overlap are calculated based on the small diameter. Therefore they are very small and can be ignored. Table 8 shows that the mass of support structures is overestimated by about 10.73% because of overlapped members. This result is similar to that shown in Kaufer et al. [20]

For the coupled natural frequencies, overlap has led to small differences (Table 9). A difference of 9.8% and 3% is found for tower modes 3 and 4, respectively.

Table 10 provides the results of three locations in terms of extremes for models with and without overlap. Overlap has a big influence on the bending moments M_y at three locations. Most of the overestimated loads vary from 2.33% to 25.61%; the decrease in bending moments M_y for member 5 is 9.18% and the decrease in M_z for member 15 is less around 8.16%.

Table 10
Extreme values due to overlap effect (kN or kNm).

Location	Load	No overlap	With overlap	Difference (%)
M5E1	F_x	−5587.8	−5812.0	4.01
	M_y	103.1	93.0	−9.80
	M_z	130.1	133.2	2.38
M15E2	F_x	−184.6	−188.9	2.33
	M_y	8.2	10.3	25.61
	M_z	−4.9	−4.5	−8.16
M132E1	F_x	−1500.8	−1590.7	5.99
	M_y	−121.9	−131.7	8.04
	M_z	93.3	98.5	5.57

Table 11
Mass comparison due to flooded effect (unit: ton).

	No flooded	With flooded	Difference (%)
Mass of support structure	1039.5	1186.0	14.09

Table 12
Tower natural frequencies due to flooded effect (unit Hz).

Mode	No flooded	With flooded	Difference (%)
1	0.2446	0.2446	0.00
2	0.2449	0.2449	0.00
3	2.0068	1.9966	−0.51
4	3.1272	3.1263	−0.03
5	3.2563	3.2535	−0.09

Table 13
Extreme values due to flooded effect (kN or kNm).

Location	Load	No flooded	With flooded	Difference (%)
M5E1	F_x	−5694.8	−6048.0	6.20
	M_y	149.0	143.7	−3.56
	M_z	149.0	152.1	2.08
M15E2	F_x	−184.3	−193.9	5.21
	M_y	10.4	10.8	3.85
	M_z	−4.6	−4.7	2.17
M132E1	F_x	−1687.4	−1670.5	−1.00
	M_y	−152.1	−161.4	6.11
	M_z	117.4	116.4	−0.85

6.3. Effect of flooding of the member

As shown in Fig. 6, water has flooded the members. For the sealed member, the mass of the enclosed water is added to the element if the member is flooded. If it is unsealed, the enclosed water is modeled as an added mass in the directions perpendicular to the element axis. Table 11 shows a mass difference of about 14.09%, which is the water mass in the flooded legs.

Table 12 summarizes the first five coupled natural frequencies for models with and without flooded members. The difference for tower modes 1 and 2 is less than 2%. The difference is limited to less than 1% for the other modes.

Because of the water in the flooded members, axial forces increase for submerged members 5 and 15 by 6.2% and 5.21%, respectively (Table 13). The bending moments vary from 0.85% to 6.11%.

6.4. Effect of marine growth

The mass of the support structure increases by 22.38% (Table 14) because of the marine growth, which cannot be ignored in the simulation.

Table 15 shows that there is no difference in the first and second tower natural frequencies after including marine growth, and a small decrease is found for other tower natural frequencies.

Table 14
Mass comparison due to marine growth effect (unit: ton).

	No marine growth	With marine growth	Difference (%)
Mass of support structure	1039.5	1272.1	22.38

Table 15
Tower natural frequencies due to marine growth effect (unit Hz).

Mode	No marine growth	With marine growth	Difference (%)
1	0.2356	0.2398	1.78
2	0.2365	0.2401	1.52
3	1.9511	1.9277	−1.20
4	3.0310	2.0625	−31.95
5	3.3895	3.4015	0.35

Table 16
Extreme values due to marine growth effect (kN or kNm).

Location	Load	No marine growth	With marine growth	Difference (%)
M5E1	F_x	−5689.7	−5890.6	3.53
	M_y	90.3	52.6	−41.75
	M_z	123.6	124.6	0.81
M15E2	F_x	−187.3	−235.2	25.57
	M_y	10.3	11.0	6.80
	M_z	−4.6	−4.8	4.35
M132E1	F_x	−1554.3	−1559.1	0.31
	M_y	−127.0	−125.8	−0.94
	M_z	99.7	99.3	−0.40

Table 17
Mass comparison due to TP mass effect (unit: ton).

	Model 1	Model 2	Model 3
Mass of TP	201.7	349.6	520.5

Table 18
Tower natural frequencies due to TP mass effect (unit Hz).

Mode	Model 1	Model 2	Model 3
1	0.2447	0.2446	0.2446
2	0.2449	0.2449	0.2448
3	2.1320	1.9966	1.808
4	3.1432	3.1263	1.8671
5	3.2684	3.2535	3.2297

The extreme values for the selected sensors are presented in Table 16 to show the marine growth effect on dynamic response. For the axial force F_x, which is the most important load for the members, marine growth led to increase varying from 0.31% to 25.57%. The largest increase occurs on the X-brace (member 15). The increase is because of the increased of diameter and the increased of roughness due to marine growth.

6.5. Effect of mass of TP

Due to different TP designs, TP mass vary significantly. This section focuses on the TP mass effect in either research-based or actually employed design concepts. Table 17 summarizes the masses for three different models. The mass of model 2 is 73.3% larger than that of model 1, and the mass of model 3 is 48.9% larger than that of model 2.

Furthermore, the first and second tower natural frequencies decrease slightly (Table 18). A larger TP mass reduces the third and fourth natural frequencies significantly.

Table 19 describes the variation in the dynamic loads with different TP masses. The large TP mass has a large effect on the member's axial force and bending moment M_y. Meanwhile, the effect is more significant for the legs than for the braces.

Compared with model 2, model 3, which has a larger mass had a smaller bending moment M_y at the seabed, showing that choosing an appropriate mass for the TP may reduce the bending moment at the seabed.

Table 19
Extreme values due to TP mass effect (kN or kNm).

Location	Load	Model 1	Model 2 (differ.)		Model 3 (differ.)	
M5E1	F_x	−5677.7	−6045.7	(6.48%)	−6237.1	(9.85%)
	M_y	98.8	143.4	(45.14%)	119.6	(21.05%)
	M_z	144.5	152.0	(5.19%)	157.6	(9.07%)
M15E2	F_x	−188.5	−193.9	(2.86%)	−225.0	(19.36%)
	M_y	10.5	10.8	(2.86%)	11.0	(4.76%)
	M_z	−4.5	−4.7	(4.44%)	−4.5	(0.00%)
M132E1	F_x	−1323.9	−1668.9	(26.06%)	−2045.6	(54.51%)
	M_y	−136.6	−162.4	(18.89%)	−173.6	(27.09%)
	M_z	115.8	116.4	(0.52%)	115.8	(0.00%)

7. Conclusions

In this work, a jacket structure was designed based on Korean Southwest Sea conditions to support a 5 MW OWT at a water depth of 33 m. In addition, the effects of different modeling parameters, including joint can, overlap, flooding the member, marine growth and TP mass, were investigated using an aero-servo-hydro-elastic simulation under Korean environmental conditions. This research provided applicable knowledge of the utilization of large-scale OWTs in Korea for intermediate water depths. The following conclusions were drawn.

1. Without joint can, the mass of the support structure was underestimated by 3.28%. A limited effect on natural frequencies was found. For extremes loads in the jacket, a joint can leads to increased extremes lying between 2.07% and 56.72%. The bending moment M_y was more sensitive to the joint can effect.
2. The mass of the support structure was overestimated by 10.73% because of overlap. Most of the loads were overestimated by between 2.33% and 25.61% for the overlap effect.
3. Flooding of the member had a small effect on the tower natural frequencies. The effect on extreme values of selected members was less than 10%.
4. For this design, the mass of marine growth was estimated as 22.4% of the support structure. There was an increase for most of extreme loads ranging from 0.31% to 25.57%.
5. In the case of the TP mass, different concepts were available according to specific and individual project requirements. Thus, the mass was different for each concept. Choosing the appropriate mass may reduce the extreme loads in the members.

Acknowledgements

This research was supported by the Human Resources Development of the Korea Institute of Energy Technology Evaluation and Planning (KETEP) grant funded by the Korea Government Ministry of Knowledge and Economy (MKE), South Korea (No 20114030200050) and also supported by the National Research Foundation of Korea (NRF) funded by the Ministry of Education, Science and Technology (grant number 2012R1A1A2008870 and 2012R1A2A2A04047240) and by Defense Acquisition Program Administration and Agency for Defense Development under the contract UD120037CD.

References

[1] Ackerman T, Söder L. Wind energy technology and current status: a review. Renew Sust Energ Rev 2000;4(4):315–74.
[2] Jan W, Marte R, Christian S, Edgar GH. Life cycle assessment of a floating offshore wind turbine. Renew Energy 2009;34(3):742–7.

[3] Jonkman JM. Dynamics of offshore floating wind turbines – model development and verification. Wind Energy 2009;12(5):459–92.
[4] Lozano-Minguez E, Kolios AJ, Brennan FP. Multi-criteria assessment of offshore wind turbine support structures. Renew Energy 2011;36:2831–7.
[5] Oh KY, Kim JY, Lee JS, Ryu KW. Wind resource assessment around Korean Peninsula for feasibility study on 100 MW class offshore wind farm. Renew Energy 2012;42:217–26.
[6] Hong L, Möller B. Offshore wind energy potential in China: under technical, spatial and economic constraints. Energy 2011;36(7):4482–91.
[7] South Korea offshore wind project plan. <http://www.evwind.es/2011/11/13/south-korea-to-build-worlds-largest-offshore-wind-farm/> [accessed 08.08.12].
[8] Thomsen JH, Forsberg T, Bittner R. Offshore wind foundations – the COWI experience. In: Proceedings of the 26th international conference on Offshore Mechanics and Arctic Engineering (OMAE), California, USA; 2007. p. 533–40.
[9] Seidel M. Feasibility of monopiles for large offshore windturbines. In: Proceedings of the 10th German Wind Energy Conference (DEWEK), Bremen, Germany; 2010.
[10] Alpha Ventus offshore wind farm. <http://www.alpha-ventus.de/index.php?id=80> [accessed 08.08.12].
[11] Beatrice wind farm demonstrator project. <http://www.beatricewind.co.uk> [accessed 06.06.12].
[12] BARD offshore 1 project. <http://www.bard-offshore.de/en/projects/offshore/bard-offshore-1.html> [accessed 08.08.12].
[13] Seidel M. Jacket substructures for the REpower5 M wind turbine. In: Proceedings of European offshore wind energy conference and exhibition, Berlin, Germany; 2007.
[14] Klose M, Dalhoff P, Argyriadis K. Integrated load and strength analysis for offshore wind turbines with jacket structures. In: Proceedings of European offshore wind energy conference and exhibition, Berlin, Germany; 2007.
[15] Gao Z, Saha NLJ, Moan T, Amdahl J. Dynamic analysis of offshore fixed windturbines under wind and wave loads using alternative computer codes. In: Proceedings of the third TORQUE conference; 2010.
[16] Dong WB, Moan T, Gao Z. Long-term fatigue analysis of multi-planar tubular joints for jacket-type offshore wind turbine in time domain. Eng Struct 2011;33(6):2002–14.
[17] Fischer T, Popko W, Soerensen JD, Kühn M. Load analysis of the upwind jacket reference support structure. In: Proceedings of DEWEK, Bremen, Germany; 2010.
[18] Moll H, Vorpahl F, Busmann H. Dynamics of support structures for offshore wind turbines in fully-coupled simulations-influence of water added mass on jacket mode shapes, natural frequencies and loads. In: Proceedings of the European wind energy conference and exhibition, Warsaw, Poland; 2010.
[19] Cordle A, Kaufer D, Vorpahl F, Fischer T, Sørensen J, Schmidt B, et al. Final report for WP4.3: enhancement of design methods and standards. UpWind deliverable D4.3.6 (WP4: offshore foundations and support structures). Garrad Hassan and Partners Ltd; 2011.
[20] Kaufer D, Fischer T, Vorpahl F, Popko W, Kühn M. Different approaches to modeling jacket support structures and their impact on overall wind turbine dynamics. In: Proceedings of the 10th German Wind Energy Conference (DEWEK), Bremen, Germany; 2010.
[21] Shi W, Park HC, Baek JH, Kim CW, Kim YC, Shin HK. Study on the marine growth effect on the dynamic response of offshore wind turbine. Int J Precis Eng Manuf 2012;13(7):1167–76.
[22] Manwell JF, McGowan JG, Rogers AL. Wind energy explained. England: John Wiley & Sons; 2004.
[23] Morison J, O'Brien M, Johnson J, Schaaf S. The force exerted by surface waves on piles. Petroleum Transactions of AIME 1950;189:149–57.
[24] Merz KO, Moe G, Gudmestad OT. A review of hydrodynamic effects on bottom-fixed offshore wind turbines. In: Proceedings of international conference on offshore mechanics and arctic engineering, Honolulu, USA; 2009.
[25] Jonkman JM, Butterfield S, Musial W, Scott G. Definition of a 5 MW reference wind turbine for offshore system development. Technical report. NREL/TP-500-38060. National Renewable Energy Laboratory; 2009.
[26] Det Norske Veritas (DNV). Design of offshore wind turbine structures. Offshore standard DNV-OS-J101; 2010.